Temperature-Dependence Corrosion Behavior of Ti6Al4V in the Presence of HCl

Fei Yu[1,2]*, Owen Addison[3] and Alison Davenport[2]

[1]Institute for Translational Medicine, The Affiliated Hospital of Qingdao University, Qingdao University, Qingdao, China, [2]School of Metallurgy and Materials, University of Birmingham, Birmingham, United Kingdom, [3]Faculty of Dentistry, Oral and Craniofacial Sciences, King's College London, London, United Kingdom

Ti alloys have been widely used in biomedical field due to good compatibility and corrosion resistance. However, corrosion-related failures of implanted Ti devices and prostheses have been regularly reported within the medical literature. The corrosion of Ti alloys has attracted much attention *in vivo* and *in vitro*. In the current study, the corrosion behavior of Ti6Al4V alloy was investigated using surface analysis and electrochemical tests. Corrosion of Ti6Al4V in 2 M hydrochloric acid is temperature dependent within the temperature range studied. It has found that the steady state current density at −510 mV vs. SCE (the primary passivation potential at the physiological temperature of 37°C) becomes higher with increasing temperature. The α phase of Ti6Al4V is preferentially dissolved relative to the β phase after potentiostatic measurement at primary passivation potential in 2 M HCl at 37°C. This investigation provides novel and useful information for Ti corrosion-related failures of biomedical implants and prostheses.

Keywords: Ti6Al4V, corrosion, temperature, HCl solution, preferential attack

1 INTRODUCTION

Increasing concern regarding the consequences of metal release from biomedical implants has stimulated efforts to better understand the conditions under which corrosion occurs, and the nature of the corrosion products that are released (Xu et al., 2018; Morrell et al., 2019; Xu et al., 2019). Oxidation-resisting steel, Co-Cr and Ti alloys are the most common biomedical implant metals in use today (Sullivan and Topoleski, 2015; Harun et al., 2017; Xu et al., 2018; Xu et al., 2019). Of these, Ti in its commercially pure and alloyed forms is mostly used for "cementless" implants because of titanium's ability to "osseointegrate" with bone, provide adequate mechanical properties, and exhibit resistance to corrosion under normal physiological conditions (Paka and Pokrowiecki, 2018; Kang and Yang, 2019; Rabadia et al., 2019; Zhang and Chen, 2019; Zhang L.-C. et al., 2020). However, there is increasing evidence to demonstrate that Ti implants do corrode in the body under specific conditions (Addison et al., 2012; Nelson et al., 2020). The combination of multiple crevice environments (metal-metal; metal-bone, metal-soft-tissue) may produce significant changes in the chemistry of the local solution which are not predicted by standard pre-clinical testing regimens (Liu et al., 2021; Smith and Gilbert, 2021). Direct evidence of Ti corrosion *in vivo* has been reported in the orthopaedic literature associated with cemented femoral stems and Morse taper connections (Jacobs et al., 1998a; Jacobs et al., 1998b; Hallam et al., 2004). These geometrical scenarios, specifically provide conditions where aggressive (acidic) chemistries may be maintained, allowing mechanically assisted crevice corrosion (MACC) to occur (Gilbert et al., 1993; Addison et al., 2012; Kubacki and Gilbert, 2021).

Several factors influence the corrosion resistance of Ti including temperature and environmental chemistry. It has been reported that the frequency of thin film breakdown events increases with increasing temperature (Kolman et al., 1998; Yu et al., 2001; Atapour et al., 2012). For biomedical applications experimental measurements are typically conducted 37°C to simulate physiological body temperature (Atapour et al., 2011) although at inflamed sites local tissue temperatures can vary by several degrees. In other applications such as dental implants, temperature fluctuations can be much larger due to ingested hot or cold foods and beverages. Within the relevant literature a range of temperatures from 25 to 50°C have been used to explore mechanistic behaviors (Jackson et al., 2000; Valero Vidal et al., 2010). Alongside temperature, the chemistry of the environment into which the implant is placed is a key factor which can influence the corrosion resistance of Ti and its alloys. In the body, Ti implants encounter a range of liquid environments which can contain components such as reactive oxygen species, or proteins which can modify corrosion resistance (Zhang et al., 2018a). Of particular importance is the presence of Cl^- in tissues fluids (100–110 mM) which reduces the passivation of Ti in acidic conditions (Mi-Kyung et al., 2015). Although an acknowledged extreme, measurement of fluids in contact with Ti alloy orthopaedic implants retrieved during revision surgery has shown that the local acidity may reach levels approaching pH 2.5 (Hallam et al., 2004). Importantly, this is an environment that represents local acidification as a consequence of MACC (Zhang et al., 2018b).

The most common Ti implant substrate in use today is the ASTM Grade V alloy, Ti6Al4V, which exhibits a microstructure containing α and β phases stabilized by Al and V, respectively (Liu et al., 2004; Yu et al., 2015; Zhang et al., 2018a). The manufacturing and processing of Ti6Al4V can be tailored to generate a variety of microstructures with different spatial distributions of the α and β phases (Atapour et al., 2010; Atapour et al., 2012). However it has been observed that these phases can have different corrosion behaviors and should corrosion occur would lead to a differential release of the alloying (Chandrasekaran et al., 2006; Atapour et al., 2011; Zhang H. et al., 2020) elements. Hence, the purpose of this study was to explore the temperature dependent corrosion behavior of Ti6Al4V in the presence of HCl and identify factors which lead to preferential corrosion of the microstructural phases. The corrosion behavior of Ti6Al4V alloy was studied in hydrochloric acid at different temperatures by applying potentiodynamic/potentionstatic polarization scans and surface analysis methods, and novel explanation can be provided regarding failure of biomedical Ti alloys.

2 MATERIALS AND METHODS

2.1 Sample Preparation

Disc-shaped test specimens (14 mm diameter and 1.2 mm thickness) were fabricated from a Ti6Al4V alloy (ASTM Grade V, Titanium Products Ltd., Solihull, United Kingdom) and the surfaces polished to a mirror finish. Polishing involved sequential use of abrasive cloths beginning with MD-Piano (Struers, Rotherham, United Kingdom) and deionized water as a lubricant, followed by MD-Largo with a 9 μm diamond suspension as a lubricant. Finally, a MD-Chem polishing cloth (Struers, Rotherham, United Kingdom) was used with 0.04 μm OP-S Colloidal Silica suspension (Struers, Rotherham, United Kingdom) to produce a mirror finish on both sides of the disc. Following polishing, specimens were thoroughly cleaned sequentially in acetone, ethanol, and deionized water using ultrasonic agitation for 10 min at each stage. Specimens were finally dried in an air stream before further experiments.

2.2 Electrochemical Tests
2.2.1 General Procedures
A standard three-electrode cell with reference electrode (RE), counter electrode (CE) and working electrode (WE) was used. The CE was a Pt mesh (working area ~4 cm^2) and RE was a commercial saturated calomel electrode (SCE). The potential was controlled with a potentiostat (ACM Instruments, United Kingdom). Ti discs were mounted in VARI-SET cold mounting acrylic (MetPrep Ltd., United Kingdom) and used as WE. The electrode was polished to a mirror surface using identical sample preparation methods. To achieve good reproducibility, the time between polishing and electrochemical measurements was controlled using the following approach throughout. After final polishing with an MD-Chem polish cloth, the samples were immediately cleaned with deionized water (Millipore), then dried in an air stream and left in open air for 5 min before immersed in the test solutions. Due to the preparatory procedures of setting up the electrochemical cell, there was a 5 min interval between the initial immersion of the sample and acquisition of the first measurement. The electrochemical cell was immersed in a water bath (Bennett Scientific Limited, Nickel Electro Ltd., England, United Kingdom) with high temperature stability (±0.5°C). The temperature was monitored with a thermocouple connected to a computer.

2.2.2 Potentiodynamic Polarization Curves
Freshly polished Ti6Al4V electrodes were immersed in 2 M HCl at 37°C. The open circuit potential (OCP) was measured for 1 h and then anodic polarization curves were measured by sweeping the potential from −50 mV below the OCP to 0 mV vs. SCE at a rate of 1 mV/s. The anodic polarization curves were measured three times for each condition, using a freshly polished sample and fresh solution in each case.

2.2.3 Potentiostatic Measurements
The corrosion behavior of Ti6Al4V in the presence of 2 M HCl was studied by potentiostatic measurements at various temperatures around the physiological norm (28°C, 31°C, 34°C, 37°C, 40°C, and 43°C). The temperature was controlled by the water bath and was recorded by a thermocouple, which was immersed in the solution. Freshly polished Ti6Al4V was immersed in 2 M HCl. OCP was measured for 30 min and then −510 mV vs. SCE was applied for 3 h. The potentiostatic

measurements were repeated three times for each condition, using a freshly polished sample and fresh solution in each case.

2.3 Surface Characterization

Ti surfaces before and after electrochemical testing were characterized using SEM. Briefly, to locate the same region on the specimen, a hardness indentation was introduced into the center of the mirror polished surface (Vickers hardness test, load: 300 g, MVK-H1 hardness testing machine, Mitutoyo, Japan). After the initial baseline measurement, the carbon layer on the surface resulting from SEM was removed by quickly (~10 s) polishing the sample on an MD-Chem polish cloth with OP-S Colloidal Silica suspension, so that it would not affect the electrochemical experiments. SEM observation was undertaken with JEOL 7000 instrument (Japan Electron Optics Laboratory Co., Ltd. accelerating voltage 20 kV, beam current ~70 μA). Both secondary electron mode (SE) and backscatter electron mode (BSE) imaging were used. Electron back-scattered diffraction (EBSD) analysis was also performed. The elemental composition of the test specimen surfaces was also analyzed by energy dispersive X-ray spectroscopy (EDX detector model: 7558 for JEOL 7000; collecting window: ATW 2; acquisition time: 60 s; quantification method: standard less; Oxford Instrument, United Kingdom).

3 RESULTS

3.1 Characterization of Ti6Al4V

Figure 1 shows the surface morphology and EDX analysis of Ti6Al4V test specimens exhibiting mirror-polished surfaces. When the "as-polished" sample was etched in Kroll's etchant (2% HF and 10% HNO_3 mixed solution) for ~5 s, the β phase was clearly observed (data not shown). Ti6Al4V surfaces show the characteristic two-phase (α and β) microstructure. Increased V and Fe was seen in the β phase and whereas the α phase contained relatively higher Al (**Figure 1C**).

3.2 Effect of HCl on Ti Corrosion
3.2.1 OCP Measurement and Anodic Polarization
Figure 2A shows the OCP as a function of time for mirror-polished Ti6Al4V in naturally-aerated 2 M HCl. The OCP started from ~−350 mV vs. SCE and then abruptly decreased to ~−670 mV vs. SCE for Ti6Al4V, indicating dissolution of the air-formed passive film and surface activation in 2 M HCl. **Figure 2B** shows that Ti6Al4V exhibited obvious active peaks during anodic polarization. The primary passivation potential (E_{pp}) of Ti6Al4V is ~−510 mV vs. SCE.

3.2.2 Temperature Dependence of Corrosion Behavior of Ti6Al4V
Figure 3 shows potentiostatic measurements of the mirror-polished Ti6Al4V in 2 M HCl at different temperatures. It shows that the steady state current density of Ti6Al4V was sensitive to temperature. It can be seen that the corrosion process at 28°C is slightly different from the behaviors above 28°C since the current density of Ti6Al4V was gradually decreased within the measured time until ~4,000 s (before reaching a relative steady state). **Figure 3C** also shows that the steady state current density of Ti6Al4V was increased with increasing temperature at above 28°C, i.e., 31°C, 34°C, 37°C, 40°C and 43°C.

3.2.3 Surface Morphology of Ti6Al4V After Potentiostatic Tests
Figure 4 and **Figure 5** compare the surface morphologies of mirror-polished Ti6Al4V before and after potentiostatic tests at −510 mV vs. SCE in 2 M HCl. It can be seen that Ti6Al4V shows a characteristic α/β two phase microstructure based on the BSE image (**Figure 4B** and **Figure 5B**) and EBSD phase map (**Figure 5A**). There is no sign of corrosion before the test (**Figure 4A**, **Figure 4B** and **Figure 5B**). However, the α phase of Ti6Al4V was found to be attacked more than the β phase after the test (**Figure 4C** and **Figure 4D**). More importantly, **Figure 5C** shows the α phase of Ti6Al4V was preferentially attacked while the β phase of Ti6Al4V stayed the same.
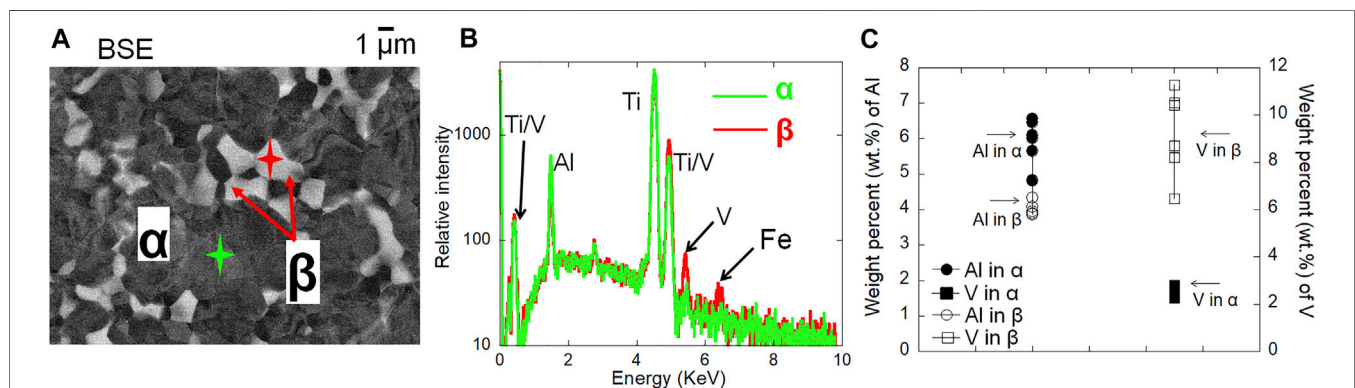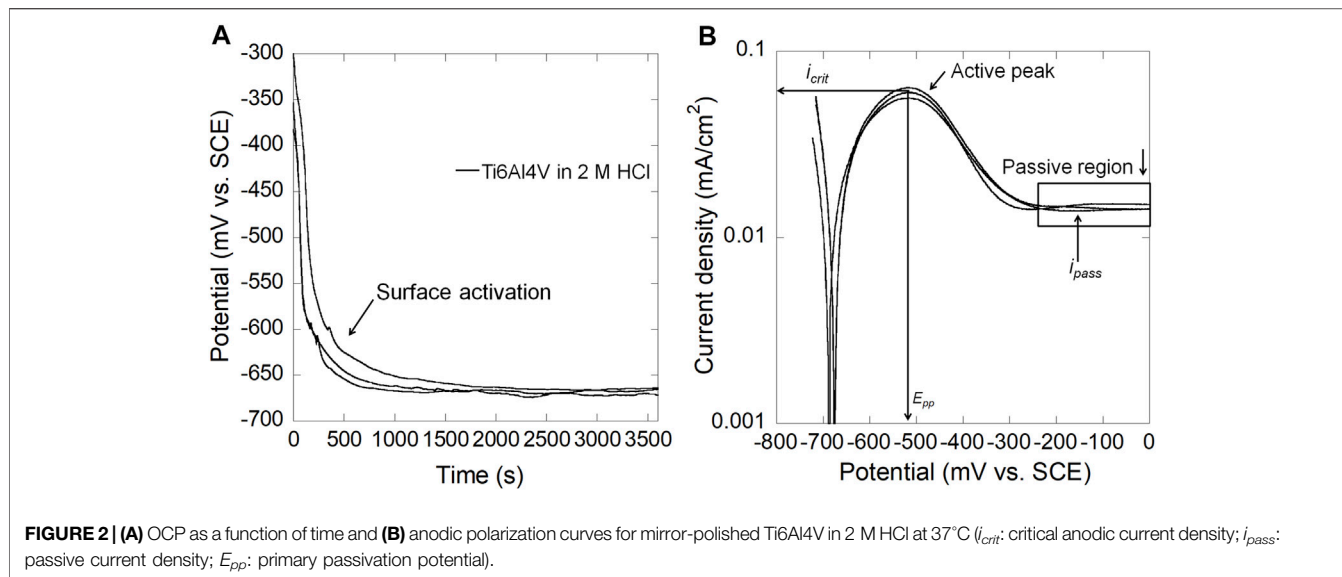

FIGURE 1 | (A) SEM, **(B)** EDX image and **(C)** weight percent (wt.%) of Al and V in α phase and β phase of mirror-polished Ti6Al4V based on the EDX analysis of randomly chosen points on the sample.

FIGURE 2 | (A) OCP as a function of time and **(B)** anodic polarization curves for mirror-polished Ti6Al4V in 2 M HCl at 37°C (i_{crit}: critical anodic current density; i_{pass}: passive current density; E_{pp}: primary passivation potential).

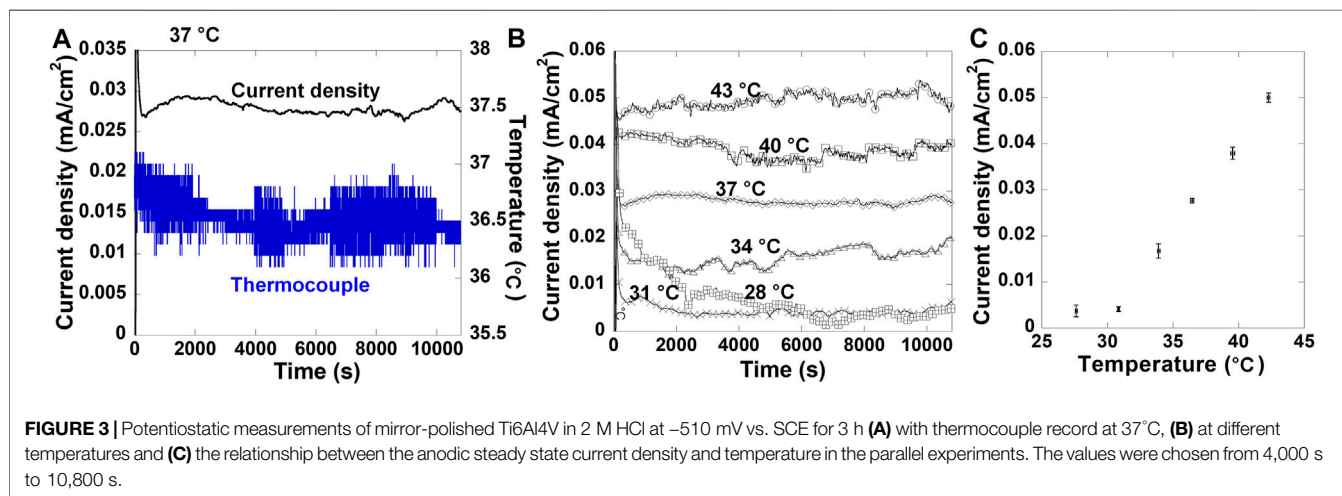## 4 DISCUSSION

4.1 Effect of HCl on Ti6Al4V Corrosion

The current study demonstrated that Ti6Al4V surfaces were activated in naturally-aerated 2 M HCl, which agrees with other studies (Atapour et al., 2010; Atapour et al., 2011). The E-pH diagram (Pourbaix diagram) at 37°C provides preliminary information about the thermodynamically stable state of Ti^{3+} within a wide range of potentials at pH < 1.5 (Yu and Scully, 1997). In the presence of 2 M HCl (pH −0.3), the OCP of Ti6Al4V was −670 mV vs. SCE (**Figure 2**), in which Ti^{3+} is the thermodynamically stable state, and therefore chemical dissolution of the Ti oxide passive film occurred as the first stage before surface activation resulting in an abrupt drop in OCP. The drop in OCP values also agreed with previous studies (Yu et al., 1999; Atapour et al., 2010; Atapour et al., 2011). In addition, a characteristic active-passive transition was observed
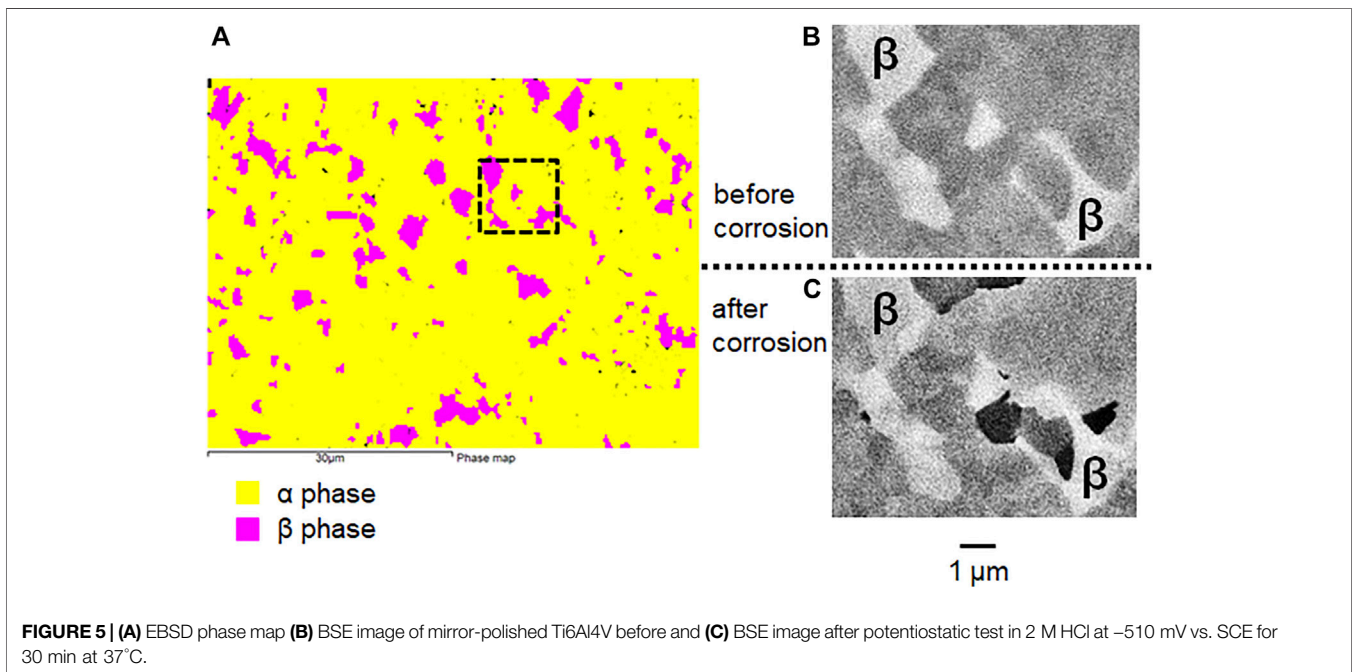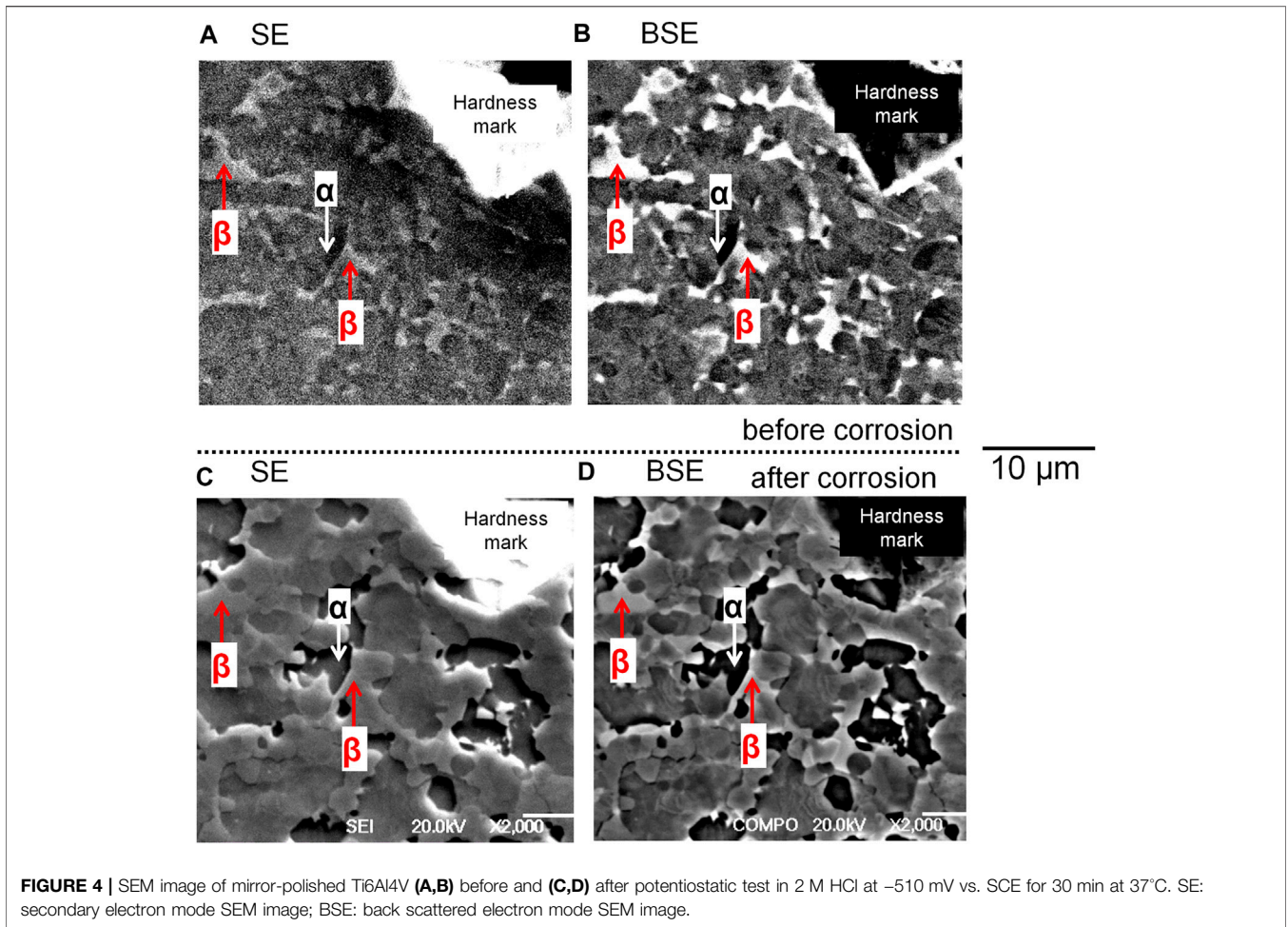
during anodic polarization in 2 M HCl. Similar E_{pp} and i_{crit} have been reported, i.e., Ti6Al4V in aerated 1.5 M HCl (Atapour et al., 2010) and in deaerated 5% (1.3 M) HCl (Atapour et al., 2012) at 37°C.
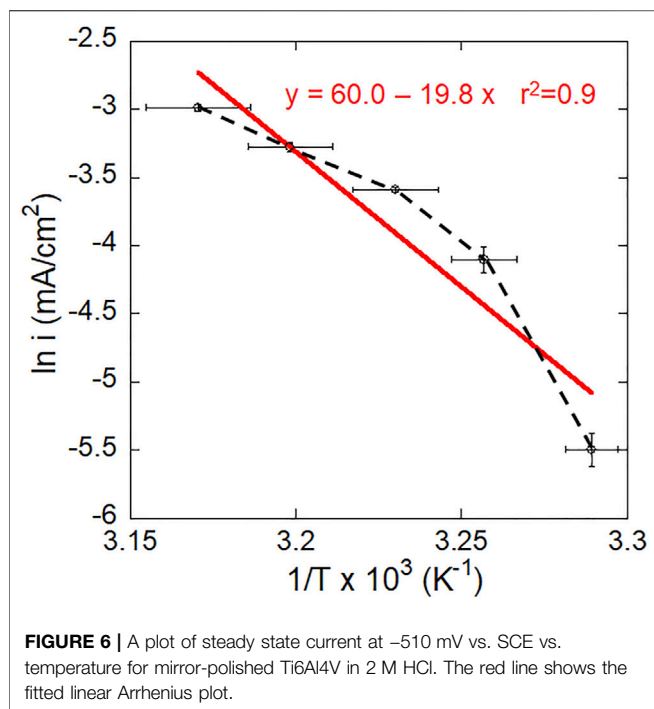
4.2 Temperature Dependence of Ti6Al4V in 2 M HCl

The steady state current density of Ti6Al4V at −510 mV vs. SCE has been observed to be increased with increasing temperature above 28°C, i.e., 31°C, 34°C, 37°C, 40 and 43°C (**Figure 3**). Assuming the corrosion process of Ti6Al4V in this study can be analyzed by a simple Arrhenius expression (**Eq. 1**) then the corrosion rate would be represented by current density:

$$\ln i = a - \frac{E_a}{RT} \qquad (1)$$

FIGURE 3 | Potentiostatic measurements of mirror-polished Ti6Al4V in 2 M HCl at −510 mV vs. SCE for 3 h **(A)** with thermocouple record at 37°C, **(B)** at different temperatures and **(C)** the relationship between the anodic steady state current density and temperature in the parallel experiments. The values were chosen from 4,000 s to 10,800 s.

FIGURE 4 | SEM image of mirror-polished Ti6Al4V **(A,B)** before and **(C,D)** after potentiostatic test in 2 M HCl at −510 mV vs. SCE for 30 min at 37°C. SE: secondary electron mode SEM image; BSE: back scattered electron mode SEM image.

FIGURE 5 | (A) EBSD phase map **(B)** BSE image of mirror-polished Ti6Al4V before and **(C)** BSE image after potentiostatic test in 2 M HCl at −510 mV vs. SCE for 30 min at 37°C.

FIGURE 6 | A plot of steady state current at −510 mV vs. SCE vs. temperature for mirror-polished Ti6Al4V in 2 M HCl. The red line shows the fitted linear Arrhenius plot.

where E_a is the activation energy of the corrosion process during potentiostatic polarization, T is the absolute temperature (K) and R is the gas constant (8.3 J/mol·K).

It can be seen from **Figure 6** that the relationship between the natural logarithm of current density and reciprocal temperature is non-linear (black line) and does not obey a linear Arrhenius expression. The corrosion processes of Ti6Al4V in this study cannot therefore be completely described in this way. However, to compare with other works, a fitted Arrhenius plot was conducted (red line) and the calculated activation energy was 164 kJ/mol.

Different activation energies have been previously reported, e.g., 27 kJ/mol by Atapour et al. (Atapour et al., 2012), 57 kJ/mol by Yu et al. (Yu et al., 1999) and 63 kJ/mol by Blackwood et al. (Blackwood et al., 1988), which may be attributed to the different methods used. The activation energy values reported by Yu et al. (Yu et al., 1999) and Blackwood et al. (Blackwood et al., 1988) are related to the dissolution/corrosion of Ti oxide on CP-Ti in deaerated 5 M HCl or 3 M H_2SO_4, respectively, and based on the surface activation time during immersion at OCP. These findings suggest that the corrosion process in this study is complicated and not controlled by a single mechanism. Active dissolution and possible passivation may co-exist since the applied potential is the primary passivation potential (−510 mV vs. SCE). In addition, the applied potential was not far from OCP (−670 mV vs. SCE), where the cathodic reaction may also take place.

4.3 Surface Morphology of Ti6Al4V After Potentiostatic Testing

The effect of microstructure on corrosion is significant, and may induce corrosion defects as a result of preferential dissolution (Zhang H. et al., 2020; Wang et al., 2022; Xu et al., 2022). The

corrosion process due to preferential attack has also been documented in the medical literature (Gilbert et al., 2012). The current study demonstrated that the α phase of Ti6Al4V was preferentially attacked relative to the β phase in 2 M HCl at 37°C after potentiostatic measurement at E_{pp} (−510 mV vs. SCE). This observation differs from Atapour's observation (Atapour et al., 2011) that the β phase of Ti6Al4V-ELI (similar to Ti6Al4V but contains lower content of C, N, O and Fe) was preferentially attacked after exposure to 5 M HCl at 37°C for 50 h. However, no over-potential was applied in Atapour's study in contrast to this report. In addition, it has been reported that the preferential dissolution of α phase of Ti-15Mo (with α+β phases microstructure) was observed at potentials in the active region in 40% H_2SO_4 at 80°C (Tomashov et al., 1974). The α phase of Ti-15Mo-3Nb-3Al was also found to be preferentially attacked during anodic polarization in 5 M HCl at 37°C (Yu and Scully, 1997).

For the Ti6Al4V used in this study, there was more Al and less V in the α phase, while there was more V but less Al in the β phase (**Figure 1**). Al has been reported to have a detrimental influence on the passivity and corrosion resistance of the α phase Ti in 5 M HCl (Yu and Scully, 1997), while dissolution of V coupled with conduction channels is also considered to be detrimental for the passive film on Ti in Hank's solution (Metikos-Hukovic et al., 2003). Considering the conditions of this study, both active dissolution and possible passivation of Ti6Al4V would be expected. The detrimental effect of Al may dominate over other factors, resulting in the observed preferential attack of α phase. It is noted that there is also some Fe content (**Figure 1**) in the β phase of Ti6Al4V in this study. Fe-containing β phase has been reported to possibly initiate hydride formation and proton reduction in acidic environment (Yan et al., 2006; Yan et al., 2011). It is likely that the cathodically active hydride sites on β phase co-exist with anodically active of α phase, which may have further resulted in the preferential dissolution of α phase.

5 CONCLUSION

In the current study, the temperature dependent corrosion behavior of Ti6Al4V has been investigated in the presence of HCl. It was found that Ti6Al4V exhibited active-passive behavior in HCl solution after surface activation. Furthermore, the steady state current density at the primary passivation potential becomes higher with increasing temperature. In addition, the factor influencing preferential corrosion of the microstructural phases has been explored. The α phase of Ti6Al4V is preferentially dissolved relative to the β phase after potentiostatic measurement. This study provides convincing evidence on preferential attack of Ti based implants and orthopedic replacements, and also supports corrosion-related failure of biomedical Ti alloys theoretically.

DATA AVAILABILITY STATEMENT

The raw data supporting the conclusion of this article will be made available by the authors, without undue reservation.

AUTHOR CONTRIBUTIONS

FY contributed to methodology, data curation, formal analysis, writing-original draft, OA contributed to writing-review and editing and supervision. AD contributed to methodology and supervision.

REFERENCES

Addison, O., Davenport, A. J., Newport, R. J., Kalra, S., Monir, M., Mosselmans, J. F. W., et al. (2012). Do 'passive' Medical Titanium Surfaces Deteriorate in Service in the Absence of Wear? *J. R. Soc. Interf.* 9 (76), 3161–3164. doi:10.1098/rsif.2012.0438

Atapour, M., Fathi, M. H., and Shamanian, M. (2012). Corrosion Behavior of Ti-6Al-4V alloy Weldment in Hydrochloric Acid. *Mater. Corrosion* 63 (2), 134–139. doi:10.1002/maco.201005821

Atapour, M., Pilchak, A., Frankel, G. S., Williams, J. C., Fathi, M. H., and Shamanian, M. (2010). Corrosion Behavior of Ti-6Al-4V with Different Thermomechanical Treatments and Microstructures. *Corrosion* 66 (6), 065004. doi:10.5006/1.3452400

Atapour, M., Pilchak, A. L., Frankel, G. S., and Williams, J. C. (2011). Corrosion Behavior of β Titanium Alloys for Biomedical Applications. *Mater. Sci. Eng. C* 31 (5), 885–891. doi:10.1016/j.msec.2011.02.005

Blackwood, D. J., Peter, L. M., and Williams, D. E. (1988). Stability and Open Circuit Breakdown of the Passive Oxide Film on Titanium. *Electrochimica Acta* 33 (8), 1143–1149. doi:10.1016/0013-4686(88)80206-8

Chandrasekaran, N., Bai, Z., and Gilbert, J. L. (2006). *Titanium Electrochemistry in the Presence of the Inflammatory Species H_2O_2*. Translation society for biomaterials annual meeting.

Gilbert, J. L., Buckley, C. A., and Jacobs, J. J. (1993). *In Vivo* corrosion of Modular Hip Prosthesis Components in Mixed and Similar Metal Combinations. The Effect of Crevice, Stress, Motion, and alloy Coupling. *J. Biomed. Mater. Res.* 27 (12), 1533–1544. doi:10.1002/jbm.820271210

Gilbert, J. L., Mali, S., Urban, R. M., Silverton, C. D., and Jacobs, J. J. (2012). *In Vivo* oxide-induced Stress Corrosion Cracking of Ti-6Al-4V in a Neck-Stem Modular Taper: Emergent Behavior in a New Mechanism of *In Vivo* Corrosion. *J. Biomed. Mater. Res.* 100B (2), 584–594. doi:10.1002/jbm.b.31943

Hallam, P., Haddad, F., and Cobb, J. (2004). Pain in the Well-Fixed, Aseptic Titanium Hip Replacement. *The J. Bone Jt. Surg. Br. volume* 86-B (1), 27–30. doi:10.1302/0301-620x.86b1.14326

Han, M.-K., Kim, J.-Y., Hwang, M.-J., Song, H.-J., and Park, Y.-J. (2015). Effect of Nb on the Microstructure, Mechanical Properties, Corrosion Behavior, and Cytotoxicity of Ti-Nb Alloys. *Materials* 8 (9), 5986–6003. doi:10.3390/ma8095287

Harun, W. S. W., Samykano, M., Lah, N. A. C., Ghani, S. A. C., Tarlochan, F., and Raza, M. R. (2017). Corrosion and Surface Modification on Biocompatible Metals: A Review. *Mater. Sci. Eng. C Mater. Biol. Appl.* 77, 1261–1274. doi:10.1016/j.msec.2017.04.102

Jackson, D. R., Omanovic, S., and Roscoe, S. G. (2000). Electrochemical Studies of the Adsorption Behavior of Serum Proteins on Titanium. *Langmuir* 16 (12), 5449–5457. doi:10.1021/la991497x

Jacobs, J. J., Gilbert, J. L., and Urban, R. M. (1998a). Corrosion of Metal Orthopaedic Implants*. *The J. Bone Jt. Surg. (American Volume)* 80 (2), 268–282. doi:10.2106/00004623-199802000-00015

Jacobs, J. J., Skipor, A. K., Patterson, L. M., Hallab, N. J., Paprosky, W. G., Black, J., et al. (1998b). Metal Release in Patients Who Have Had a Primary Total Hip Arthroplasty. A Prospective, Controlled, Longitudinal Study*. *J. Bone Jt. Surg.* 80 (10), 1447–1458. doi:10.2106/00004623-199810000-00006

Kang, L., and Yang, C. (2019). A Review on High-Strength Titanium Alloys: Microstructure, Strengthening, and Properties. *Adv. Eng. Mater.* 21, 1801359. doi:10.1002/adem.201801359

Kolman, D. G., Gaudett, M. A., and Scully, J. R. (1998). Modeling of Anodic Current Transients Resulting from Oxide Rupture of Plastically Strained β + α Titanium. *J. Electrochem. Soc.* 145 (6), 1829–1840. doi:10.1149/1.1838564

FUNDING

Kubacki, G. W., and Gilbert, J. L. (2021). The Effect of Hypochlorous Acid on the Tribocorrosion of CoCrMo/Ti-6Al-4V Bearing Couples. *J. Biomed. Mater. Res.* 109 (12), 2536–2544. doi:10.1002/jbm.a.37248

Liu, X., Chu, P., and Ding, C. (2004). Surface Modification of Titanium, Titanium Alloys, and Related Materials for Biomedical Applications. *Mater. Sci. Eng. R: Rep.* 47 (3-4), 49–121. doi:10.1016/j.mser.2004.11.001

Liu, Y., Zhu, D., and Gilbert, J. L. (2021). Sub-nano to Nanometer Wear and Tribocorrosion of Titanium Oxide-Metal Surfaces by *In Situ* Atomic Force Microscopy. *Acta Biomater.* 126, 477–484. doi:10.1016/j.actbio.2021.03.049

Metikos-Hukovic, M., Kwokal, A., and Piljac, J. (2003). The Influence of Niobium and Vanadium on Passivity of Titanium-Based Implants in Physiological Solution. *Biomaterials* 24 (21), 3765–3775. doi:10.1016/s0142-9612(03)00252-7

Morrell, A. P., Floyd, H., W. Mosselmans, J. F., Grover, L. M., Castillo-Michel, H., Davis, E. T., et al. (2019). Improving Our Understanding of Metal Implant Failures: Multiscale Chemical Imaging of Exogenous Metals in *Ex-Vivo* Biological Tissues. *Acta Biomater.* 98, 284–293. doi:10.1016/j.actbio.2019.05.071

Nelson, K., Hesse, B., Addison, O., Morrell, A. P., Gross, C., Lagrange, A., et al. (2020). Distribution and Chemical Speciation of Exogenous Micro- and Nanoparticles in Inflamed Soft Tissue Adjacent to Titanium and Ceramic Dental Implants. *Anal. Chem.* 92 (21), 14432–14443. doi:10.1021/acs.analchem.0c02416

Pałka, K., and Pokrowiecki, R. (2018). Porous Titanium Implants: A Review. *Adv. Eng. Mater.* 20, 1700648. 1700648. doi:10.1002/adem.201700648

Rabadia, C. D., Liu, Y. J., Chen, L. Y., Jawed, S. F., Wang, L. Q., Sun, H., et al. (2019). Deformation and Strength Characteristics of Laves Phases in Titanium Alloys. *Mater. Des.* 179, 107891. doi:10.1016/j.matdes.2019.107891

Smith, S. M., and Gilbert, J. L. (2021). Interfacial Compliance, Energy Dissipation, Frequency Effects, and Long-term Fretting Corrosion Performance of Ti-6Al-4V/CoCrMo Interfaces. *J. Biomed. Mater. Res* 110, 409–423. doi:10.1002/jbm.a.37299

Sullivan, S. J. L., and Topoleski, L. D. T. (2015). Surface Modifications for Improved Wear Performance in Artificial Joints: A Review. *Jom* 67 (11), 2502–2517. doi:10.1007/s11837-015-1543-0

Tomashov, N. D., Chernova, G. P., Ruscol, Y. S., and Ayuyan, G. A. (1974). The Passivation of Alloys on Titanium Bases. *Electrochimica Acta* 19 (4), 159–172. doi:10.1016/0013-4686(74)85012-7

Valero Vidal, C., Olmo Juan, A., and Igual Muñoz, A. (2010). Adsorption of Bovine Serum Albumin on CoCrMo Surface: Effect of Temperature and Protein Concentration. *Colloids Surf. B: Biointerfaces* 80 (1), 1–11. doi:10.1016/j.colsurfb.2010.05.005

Wang, J., Zhang, B., Xu, W., Zhang, J., Yang, L., Peng, Z., et al. (2022). Microstructure Refinement on Crevice Corrosion of High-Speed Rail Steel U75V Visualized by an *In Situ* Monitoring System. *Front. Mater.* 8. doi:10.3389/fmats.2021.820721

Xu, W., Deng, Y., Zhang, B., Zhang, J., Peng, Z., Hou, B., et al. (2022). Crevice Corrosion of U75V High-Speed Rail Steel with Varying Crevice gap Size by *In-Situ* Monitoring. *J. Mater. Res. Tech.* 16, 1856–1874. doi:10.1016/j.jmrt.2021.12.116

Xu, W., Yu, F., Yang, L., Zhang, B., Hou, B., and Li, Y. (2018). Accelerated Corrosion of 316L Stainless Steel in Simulated Body Fluids in the Presence of H2O2 and Albumin. *Mater. Sci. Eng. C* 92, 11–19. doi:10.1016/j.msec.2018.06.023

Xu, W., Zhang, B., Yang, L., Ni, Q., Li, Y., and Yu, F. (2019). Effect of the Coexistence of Albumin and H2O2on the Corrosion of Biomedical Cobalt Alloys in Physiological saline. *RSC Adv.* 9 (57), 32954–32965. doi:10.1039/c9ra05699h

Yan, L., Noël, J. J., and Shoesmith, D. W. (2011). Hydrogen Absorption into Grade-2 Titanium during Crevice Corrosion. *Electrochimica Acta* 56 (4), 1810–1822. doi:10.1016/j.electacta.2010.11.017

Yan, L., Ramamurthy, S., Noël, J. J., and Shoesmith, D. W. (2006). Hydrogen Absorption into Alpha Titanium in Acidic Solutions. *Electrochimica Acta* 52 (3), 1169–1181. doi:10.1016/j.electacta.2006.07.017

Yu, F., Addison, O., and Davenport, A. J. (2015). A Synergistic Effect of Albumin and H₂O₂ Accelerates Corrosion of Ti6Al4V. *Acta Biomater.* 26, 355–365. doi:10.1016/j.actbio.2015.07.046

Yu, S. Y., Brodrick, C. W., Ryan, M. P., and Scully, J. R. (1999). Effects of Nb and Zr Alloying Additions on the Activation Behavior of Ti in Hydrochloric Acid. *J. Electrochem. Soc.* 146 (12), 4429–4438. doi:10.1149/1.1392655

Yu, S. Y., and Scully, J. R. (1997). Corrosion and Passivity of Ti-13% Nb-13% Zr in Comparison to Other Biomedical Implant Alloys. *Corrosion* 53 (12), 965–976. doi:10.5006/1.3290281

Yu, S. Y., Scully, J. R., and Vitus, C. M. (2001). Influence of Niobium and Zirconium Alloying Additions on the Anodic Dissolution Behavior of Activated Titanium in HCl Solutions. *J. Electrochem. Soc.* 148 (2), B68–B78. doi:10.1149/1.1337605

Zhang, H., Man, C., Wang, L., Dong, C., Wang, L., Kong, D., et al. (2020a). Different Corrosion Behaviors between α and β Phases of Ti6Al4V in Fluoride-Containing Solutions: Influence of Alloying Element Al. *Corrosion Sci.* 169, 108605. doi:10.1016/j.corsci.2020.108605

Zhang, L.-C., Chen, L.-Y., and Wang, L. (2020b). Surface Modification of Titanium and Titanium Alloys: Technologies, Developments, and Future Interests. *Adv. Eng. Mater.* 22 (5), 1901258. doi:10.1002/adem.201901258

Zhang, L. C., and Chen, L. Y. (2019). A Review on Biomedical Titanium Alloys: Recent Progress and Prospect. *Adv. Eng. Mater.* 21 (4), 1801215. doi:10.1002/adem.201801215

Zhang, Y., Addison, O., Yu, F., Troconis, B. C. R., Scully, J. R., and Davenport, A. J. (2018a). Time-dependent Enhanced Corrosion of Ti6Al4V in the Presence of H₂O₂ and Albumin. *Sci. Rep.* 8. doi:10.1038/s41598-018-21332-x

Zhang, Y., Davenport, A. J., Burke, B., Vyas, N., and Addison, O. (2018b). Effect of Zr Addition on the Corrosion of Ti in Acidic and Reactive Oxygen Species (ROS)-Containing Environments. *ACS Biomater. Sci. Eng.* 4 (3), 1103–1111. doi:10.1021/acsbiomaterials.7b00882